PHYSICAL REVIEW B VOLUME 24, NUMBER 5 1 SEPTEMBER 1981

Study of local environment in a series of amorphous ferric fluorides

M. Eibschütz, M. E. Lines, L. G. Van Uitert, H. J. Guggenheim, and G. J. Zydzik
Bell Laboratories, Murray Hill, New Jersey 07974

(Received 24 April 1981)

Amorphous samples of FeF_3, $KFeF_4$, and $RbFeF_4$ have been prepared by vapor deposition at liquid-nitrogen temperature, and room-temperature Mössbauer quadrupole spectra are reported for each. The spectra are broad and indicate the existence of a distribution of electric-field-gradient (EFG) magnitudes at the iron sites. Using a least-squares computer fit to the data determined from a Lorentz broadened EFG distribution function, we are able to make separate determinations of the Lorentz widths of the individual transitions and of the form of the EFG distribution. We find a natural Lorentz width of 0.20 mm/s and an EFG distribution function of asymmetric Gaussian form. The latter has the same shape for all three materials and is both significantly broader and more asymmetric about its peak than predicted by random-packing models using hard spheres and point-charge summations. An analytic shell-model distribution function is shown to be an accurate description of EFG histograms for random-packing models but is unable to provide a quantitative description of the measured quadrupole spectra.

I. INTRODUCTION

Iron Mössbauer quadrupole spectroscopy in amorphous magnetic insulators provides a valuable probe of local environment via the coupling of the nuclear quadrupole of the Mössbauer level to the electric-field gradient (EFG) at the iron sites. Although detailed inferences on the characteristics of the local iron coordination can be obtained only indirectly, via comparison with specific models, general features of the spectra, such as the magnitude of the quadrupole splitting (QS) and the linewidths, already carry information sufficient to point the way to plausible models for this class of materials.

In the amorphous ferric fluorides, for example, the fact that the quadrupole splittings bear no relation whatsoever to their respective crystalline values[1] immediately argues against any model which contains strongly directional bonds. Chemically, since the ferric ion ($3d^5$) is spherical and the fluorines are very strongly electronegative, a model using the technique of random-packing hard spheres (RPHS)[2–4] of appropriate sizes is thought to be fairly realistic, and early results using computer-generated RPHS models in the context of amorphous magnetic insulators has been encouraging.[5–7] The RPHS predictions for QS and linewidth have been qualitatively in accord with experiment but quantitative comparisons have not yet been possible due both to the insufficient statistical accuracy of the models and sometimes of the Mössbauer data itself. The model difficulties arise from computer time and expense limitations on the size of the generated clusters.

In this paper we report measurements of ^{57}Fe Mössbauer quadrupole spectra in a series of amorphous ferric fluorides which are of sufficient accuracy to enable a separate determination to be made of the Lorentz widths of the individual transitions making up the spectra and the width and degree of asymmetry of the EFG distribution at the iron sites. We also report greatly improved computer simulations of RPHS field gradient distributions and verify the essential validity (in the RPHS context) of an analytic form recently proposed from "shell model" studies.[8] Our primary conclusion, fitting a Lorentz broadened shell distribution to the quadrupole spectra, is that the RPHS field gradient model (at least in its hard sphere form) is not a quantitative representation for these amorphous magnetic insulators.

Mössbauer data are presented for the amorphous series a-FeF_3, a-$KFeF_4$, and a-$RbFeF_4$ and are computer analyzed, using a nonlinear least-squares-fitting procedure, in terms of Lorentz broadened EFG distributions. We find in all three materials that the Lorentz linewidth is very close to the natural linewidth of 0.20 mm/s but that the EFG distributions are considerably broader and more asymmetric than predicted by RPHS models. Approximate fits to RPHS distributions using Lorentz widths up to two times their natural values, although entertained as a possibility in earlier analyses of less accurate FeF_3 Mössbauer data,[7] can now be excluded. It follows that the random packing hard sphere models, though almost certainly applicable in principle in the context of amorphous ferric insulators, are at best only qualitative in their field gradient predictions for these materials. Whether this is truly an inaccuracy in their representation of local environment, or whether it results from point charge simplifications made in the computation of EFG sums, remains to be determined.

II. EXPERIMENTAL

Amorphous ferric fluorides FeF_3, $KFeF_4$, and $RbFeF_4$ were deposited as films by evaporation of the respective crystalline materials onto both graphite and boron nitride substrates. FeF_3 was also deposited on a glass substrate. A $\frac{3}{4}$-inch-diameter graphite or boron nitride rod was sliced to form disks of 25-mil thickness. These were hand lapped to 12 mils on emery paper. A copper block substrate holder which could be cooled with liquid nitrogen and could hold two $\frac{3}{4}$-inch-diameter samples at a time was constructed. The block was installed approximately 9 in. above a boat position in a standard evaporation unit.

The substrates were held to the block by aluminum-filled epoxy (epotech) but without adding the hardener so that the samples could easily be removed later. The fluorides were evaporated onto the substrate and films of approximately 50 000 Å were obtained in 3 h. The station was first pumped for 24 h to a pressure of 1.2×10^{-6} torr in order to remove all traces of moisture. Liquid nitrogen was then passed through the block and evaporation initiated. At the end of the run the evaporator was flushed with dry nitrogen and the samples quickly placed in a dry-nitrogen-filled bottle for removal to a dry-nitrogen-filled dry box. Here the epoxy film was removed using Q tips dipped into acetone to wipe the back of the substrate surface. The samples were then mounted in a plastic sample holder and sealed before removal from the dry box.

The ^{57}Fe Mössbauer absorption spectra were obtained in a standard transmission geometry using a conventional constant acceleration spectrometer and a ^{57}Co-in-Pd source. The room-temperature Mössbauer spectra for all three materials deposited on graphite are shown in Fig. 1. The Mössbauer spectra for the fluorides deposited on boron nitride (and for the FeF_3 sample deposited on glass) are identical, within the statistical scatter of the data, to their graphite substrate equivalents.

The Mössbauer spectrum for each material shows two resonance absorption lines due to a nonzero electric field gradient at the iron sites. The linewidths are broad with full widths at half maximum of 0.41, 0.53, and 0.50 (mm/s) for FeF_3, $KFeF_4$, and $RbFeF_4$, respectively. The broad linewidths are indicative of a distribution of electric field gradients. The peak-to-peak quadrupole splitting and isomer-shift data are shown for each amorphous material in Table I where the values are compared with their crystalline equivalents.

The isomer-shift data indicate that the iron in the amorphous samples is in the Fe^{3+} valence state. We note that our value of 0.45 mm/s for amorphous FeF_3 is slightly smaller than the 0.54-mm/s value reported by Ferey *et al.*[9] for this same material. Both values, however, would indicate a ferric state for the constituent iron atoms. The amorphous Mössbauer spectra are to be contrasted with their single-crystal equivalents.[10–12] Crystalline FeF_3 has a long-range magnetic order at room temperature and thereby exhibits a six-line Zeeman-split spectrum. In its paramagnetic phase crystalline FeF_3 exhibits a

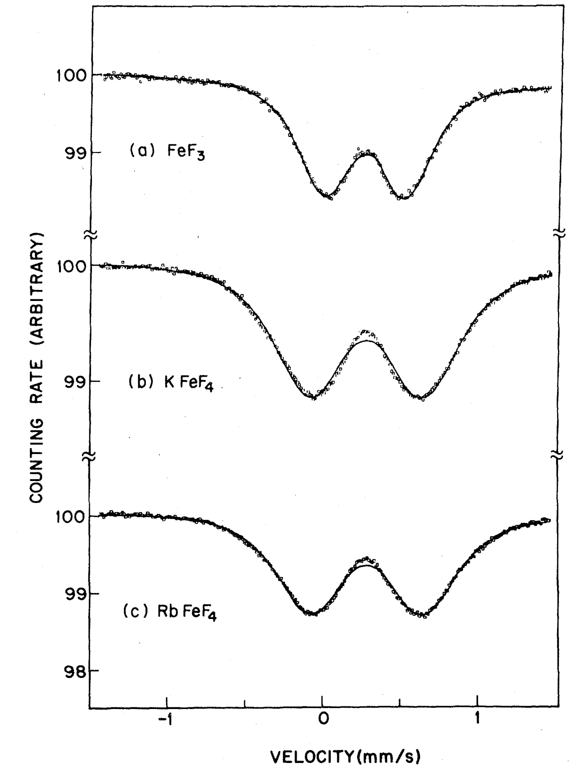

FIG. 1. Room-temperature Mössbauer spectra for the amorphous fluorides FeF_3, $KFeF_4$, and $RbFeF_4$. The solid lines represent least-squares fits to the data using the "shell model" as described in the text.

TABLE I. Room-temperature Mössbauer-effect parameters for the three amorphous ferric fluorides and their crystalline counterparts. The Isomer shift is with respect to iron metal at room temperature.

		Peak-to-peak quadrupole splitting (mm/s)	Isomer shift (mm/s)
FeF_3	Amorphous	0.55	0.45
	Crystalline	0	0.489[a]
$KFeF_4$	Amorphous	0.75	0.45
	Crystalline	1.50[b]	0.45[b]
$RbFeF_4$	Amorphous	0.75	0.46
	Crystalline	1.60[c]	0.47[c]

[a] From Ref. 10. [b] From Ref. 11. [c] From Ref. 12.

single-line spectrum indicating a zero or negligibly small quadrupole splitting. Crystalline $KFeF_4$ and $RbFeF_4$ are quasi-two-dimensional materials with large electric field gradients at the iron sites. They are paramagnetic at room temperature and each exhibits a pair of narrow quadrupole-split lines with a peak-to-peak separation ~ 1.5 mm/s which is about twice the value observed for their amorphous equivalents.

If our materials were microcrystalline we should therefore expect either a single line (if the Curie temperature were depressed below room temperature by the microcrystallinity) or a six-line Mössbauer pattern for FeF_3 and quadrupole split doublets for $KFeF_4$ and $RbFeF_4$ with a splitting close to twice that actually observed. It follows that the Mössbauer effect for ferric materials is an effective tool for the detection of the amorphous state.

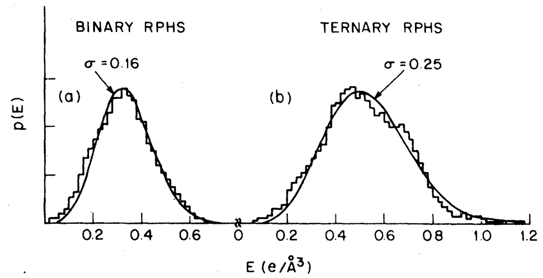

FIG. 2. (a) Computer generated histogram for the quadrupole energy distribution at iron sites in a RPHS binary amorphous aggregate (actually FeF_3, see text); the full curve is the best fit to the histogram using the shell distribution function Eq. (3.3) and has a distribution width parameter $\sigma = 0.16\ e/\text{Å}^3$. (b) As (a) but for a ternary amorphous aggregate (actually YIG, see text); the full curve is again the fit to Eq. (3.3) this time with a width parameter $\sigma = 0.25\ e/\text{Å}^3$.

III. RANDOM-PACKING MODELS

Computer-generated aggregates, using a basic RPHS technique, have been reported previously[5,7] for amorphous magnetic insulators; specifically for *a*-YIG (yttrium iron garnet) and for *a*-FeF_3. However, with only of order 800 spheres per aggregate, significant problems were encountered in finding an accurate EFG distribution because of the boundary truncation errors in the point-charge summation. Only a relatively few iron spheres near the cluster center could be sampled with confidence in this respect and the statistical accuracy was therefore relatively poor.

The computer models were considered using a basic method involving the sequential addition of hard spheres[3,4] but with the additional requirement that ions of like charge be separated as far as possible within the basic building algorithm. This latter requirement, essential for materials in which Coulomb forces between charged "ions" are playing an important role, tends to minimize the local Coulomb energy.

With access to a Cray-1 computer we have now been able to increase the cluster sizes to 2221 spheres for *a*-FeF_3 and 2555 spheres for *a*-YIG. Building procedures are exactly as set out in the earlier papers[5,7] the only change being the continuation of building from ~ 800 to more than 2000 spheres. Using formal valence point charges and sampling only iron sites which are at least 7 Å from the surface of the cluster we find new EFG histograms [or more exactly quadrupolar energy distributions $p(E)$ as defined below[13]] as shown in Figs. 2(a) and 2(b). The *a*-FeF_3 and *a*-YIG distributions are of different widths on an absolute scale (due primarily to the differences in formal charges on the ions) but they are obviously very similar in shape, a shape which may therefore be taken to be representative of both binary and ternary RPHS structures.

An analytic form for this distribution $p(E)$ has recently been proposed by Czjzek *et al.*[8] Using a model consisting of randomly positioned spheres constrained to a spherical shell around the site of interest, they are able to deduce an analytic form for the full EFG distribution as follows:

$$p(q,\eta) \sim (q/\sigma)^4 \eta (1-\eta^2/9) \times \exp[-q^2(1+\eta^2/3)/2\sigma^2] \ , \qquad (3.1)$$

in which $q = eV_{zz}$ is the primary component of EFG, $\eta = |(V_{xx}-V_{yy})/V_{zz}|$ is the orthorhombic asymmetry parameter, and σ is a parameter defining the width of the distribution. They suggest, because of the tendency of spheres to cluster into shells in RPHS models, that the form (3.1) may well be a good approximation for actual RPHS structures.

At any particular iron site the Mössbauer quadrupole resonance actually measures an energy[14]

$$E \propto |q(1+\eta^2/3)^{1/2}| \ , \qquad (3.2)$$

in terms of which the distribution (3.1) is separable in the form $p(E,\eta) = p(E)p(\eta)$ where

$$p(E) = A(E/\sigma)^4 \exp(-E^2/2\sigma^2) \ , \qquad (3.3)$$

in which A is an amplitude parameter which can be expressed in terms of σ if the distribution is normalized.

In Figs. 2(a) and 2(b) we show fits of the "shell function" (3.3) to the RPHS computer histograms for this same distribution function $p(E)$. Since the theoretical function is completely determined once the position of its peak is fixed, the fits to the RPHS histograms are impressive and establish that the shell function is a good representation for actual RPHS structures. Equally good fits to the histograms can be obtained using asymmetric Gaussian forms (as is assumed in Refs. 5–7) but this formalism has two additional adjustable parameters (the half-widths above and below the peak) and is wholly heuristic. The main conclusion of this section is therefore that the shell function (3.3) gives an accurate measure of the width (relative to the peak) of the RPHS models.

IV. ANALYSIS OF THE EXPERIMENTAL RESULTS

For an EFG distribution $p(E)$, where E is given by Eq. (3.2), we can in general express the quadrupole doublet line shape $f(z)$ as a distribution of Lorentzian lines in the form

$$f(z)=h\int_{-\infty}^{\infty}\frac{(w/2)^2p(E)}{(w/2)^2+(z-y)^2}\,dy\ , \qquad (4.1)$$

in which $E=|y-\delta|$ (where δ is the isomer shift), w is the full Lorentzian width at half-height, and h is an amplitude parameter. The equation (4.1) describes a completely symmetric doublet centered at $z=\delta$ and with a lineshape determined by the EFG distribution $p(E)$.

To interpret the observed quadrupole doublet spectra of Figs. 1 and 3 we try first a distribution $p(E)$ of shell form [Eq. (3.3)]. We compute $f(z)$ numerically in the form

$$f(z)=h_-\int_{-\infty}^{\delta}\frac{(w_-/2)^2p(|y-\delta|)}{(w_-/2)^2+(z-y)^2}\,dy$$

$$+h_+\int_{\delta}^{\infty}\frac{(w_+/2)^2p(|y-\delta|)}{(w_+/2)^2+(z-y)^2}\,dy\ , \qquad (4.2)$$

where we have allowed the amplitude (h_+,h_-) and Lorentz linewidth (w_+,w_-) to float separately in the two halves of the doublet to allow us to monitor in a formal manner any small asymmetry which may be present (due perhaps to a small correlation between isomer shift and EFG). In fact, asymmetry of this type is extremely small in the present spectra.

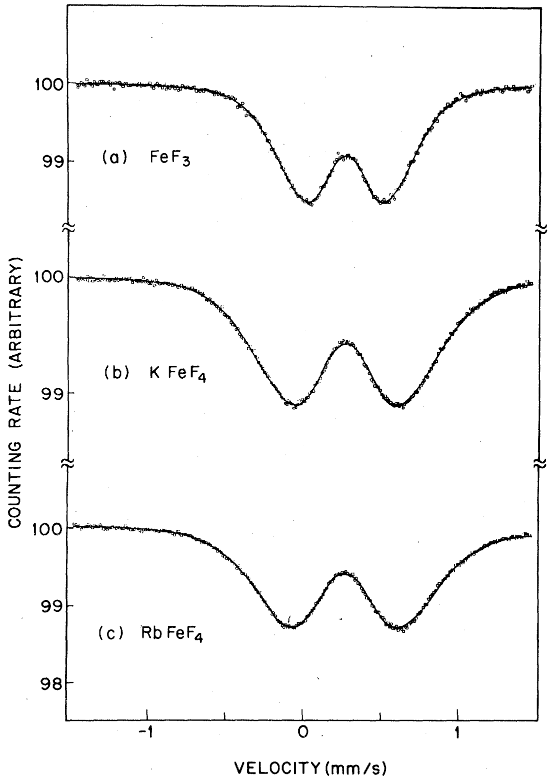

FIG. 3. (a)–(c) Same Mössbauer data as in Fig. 1 but now fitted (solid lines) by a least-squares procedure based on an asymmetric Gaussian distribution of electric field gradients (see text).

TABLE II. Quadrupole splitting model parameters, as defined in the text, determined by nonlinear-least-squares fitting to the Mössbauer data. Parameters h_+/h_-, a, b, and ϕ are dimensionless, the rest are in mm/s. ϕ is a rms deviation parameter measuring quality of fit.

Shell model	a-FeF$_3$	a-KFeF$_4$	a-RbFeF$_4$
h_+/h_-	1.015	1.016	1.006
w_-	0.33	0.39	0.34
w_+	0.31	0.38	0.34
σ	0.130	0.176	0.179
ϕ	0.220×10^{-4}	0.202×10^{-4}	0.239×10^{-4}
δ	0.450	0.453	0.462
Asymmetric Gaussian model			
h_+/h_-	1.057	1.025	0.982
w_-	0.23	0.22	0.20
w_+	0.20	0.21	0.22
a	0.59	0.61	0.57
b	1.07	1.19	1.10
D	0.223	0.295	0.303
ϕ	0.150×10^{-4}	0.651×10^{-5}	0.108×10^{-4}
δ	0.451	0.453	0.461

Computer fitting the form (4.2) to the experimental data for the three amorphous materials a-FeF$_3$, a-KFeF$_4$, and a-RbFeF$_4$ using a nonlinear-least-squares program we find the best "shell-model" fits as shown in Figs. 1(a), 1(b), and 1(c). The corresponding best-fit parameter values are given in Table II. Visually the best fit is for a-FeF$_3$ but the fit is obviously less than quantitative for the other two materials. From our standpoint the most significant finding is that each of the shell-model fits to the Mössbauer data calls for large Lorentz widths (between 0.31 and 0.39 mm/s, values which are from 1.5 to 2 times the natural linewidth 0.20 mm/s). Although such Lorentz widths are not unknown for thick crystalline samples[15] they are expected to be much closer to natural linewidth for very thin samples of the kind used in the present experiments.

The width of each of the Mössbauer doublet lines is essentially the sum of the widths of the EFG distribution and the Lorentz contribution. Since the shell function (3.3) cannot vary its width independently of its peak the "best-fit" Lorentzian widths w in this model are forced by the fit to the peak separation. We would much prefer to analyze each line shape separately to deduce the degree of Lorentz character in the wings in order to get an independent estimate of Lorentz width w. This can be done by choosing an EFG distribution function which is basically "shell-like" but which can independently vary its peak position and its width.

For this purpose we use a $p(E)$ of asymmetric Gaussian form

$$p(E)=\begin{cases} p_1(E-D)=\exp\{-[(E-D)/aD]^2\}, & 0<E<D \\ p_2(E-D)=\exp\{-[(E-D)/bD]^2\}, & D<E<\infty\ . \end{cases} \tag{4.3}$$

in which D measures the peak of the distribution, and the dimensionless parameters a and b determine the asymmetric half-widths. This function, for $D=2\sigma$, $a=0.45$, $b=0.53$ can mimic the "shell function" distribution very well (see Fig. 4) but it also allows us the freedom of varying the distribution width (i.e., a and b) independently of the position D of the peak, which controls the quadrupole splitting. Using the asymmetric Gaussian (4.3) we compute the QS line shapes in the form

$$f(z)=h_-\left[\int_{-\infty}^{\delta-D} F_2^-\,dy+\int_{\delta-D}^{\delta} F_1^-\,dy\right] + h_+\left[\int_{\delta}^{\delta+D} F_1^+\,dy+\int_{\delta+D}^{\infty} F_2^+\,dy\right]\ , \tag{4.4}$$

where

$$F_i^{\pm}=\frac{(w_\pm/2)^2 p_i(y-\delta\mp D)}{(w_\pm/2)^2+(z-y)^2},\quad i=1,2\ . \tag{4.5}$$

Using this formalism the new best fits to the Mössbauer quadrupole data are shown in Figs. 3(a), 3(b), 3(c). The corresponding best-fit parameter values are given in Table II. The fits to the data are now essentially quantitative for all three materials. An improvement over the shell model is, of course, not surprising since we now have two additional variables. The significant point is that for each QS spectrum the Lorentz width (independent of its initial values in the nonlinear least-squares-fitting iteration) settles down very close indeed to its natural value of 0.20 mm/s. This indicates that the wings of the Mössbauer lines have a degree of Lorentzian character, for all three materials, which requires a quasinatural linewidth for its quantitative interpretation.

This being so, it now follows that the EFG linewidth must be correspondingly greater than the shell-model width. From Table II we see that, although the EFG peak occurs at an energy D which is quite different for a-FeF$_3$ on the one hand and a-KFeF$_4$ and a-RbFeF$_4$ on the other, the *shape* of the EFG distribution in each case (as measured by the parameters a and b) is essentially the same with $a=0.59\pm0.02$ and $b=1.12\pm0.07$. In Fig. 5 we compare this best-fit asymmetric Gaussian solution from Table II with the equivalent best shell-model fit. We conclude that the shell model, and as the result of the findings of Sec. III the RPHS model itself, has an EFG distribution width which is smaller than ex-

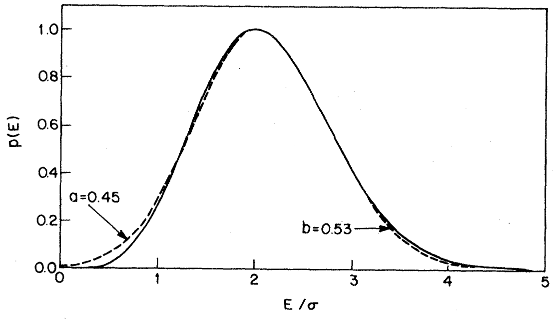

FIG. 4. Full curve is the shell distribution function Eq. (3.3) of the text. The dashed curve demonstrates the extent to which it can be mimicked by the asymmetric Gaussian distribution Eq. (4.3) if the Gaussian parameters are correctly chosen; namely, $D=2\sigma$, $a=0.45$, and $b=0.53$.

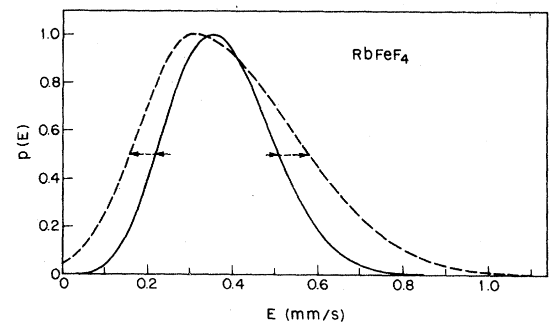

FIG. 5. Comparison of the "best-fit" shell distribution function (solid curve) to the "best-fit" asymmetric Gaussian (dashed curve) for the electric field gradient distribution function in the amorphous fluorides. The energy scale corresponds to a-KFeF$_4$ or a-RbFeF$_4$ and should be reduced by 25% in order to quantitatively represent a-FeF$_3$. The asymmetric Gaussian distribution, which the work of this paper indicates is close to the actual EFG distribution in these materials, has a full width at half-height (see arrows) which exceeds that for the shell model by some 45%.

periment by some 30% and a distribution shape which is too symmetric about its peak. Although the asymmetric Gaussian form is purely heuristic and has some features (e.g., a nonzero value as $q \to 0$) which are possibly spurious, it is evidently a good semiquantitative representation for the amorphous ferric fluorides.

V. SUMMARY

We have prepared amorphous samples of the three ferric fluorides FeF_3, $KFeF_4$, and $RbFeF_4$ and report room-temperature ^{57}Fe Mössbauer measurements for each of them. The spectra are very broad doublets with linewidths of order 70% of the peak-to-peak splitting in each case. After establishing the validity of an analytic EFG distribution function, termed the shell model, for computer aggregates of randomly packed binary and ternary hard sphere models of amorphous magnetic insulators, we attempt a fit to the Mössbauer spectra using this model. We find that a Lorentz broadened shell-model function is unable to quantitatively reproduce the data and conclude that the dense random packing model is at best only qualitatively valid for these materials.

The Mössbauer data are sufficiently accurate to enable us to make an independent determination of the Lorentz linewidth of the individual transitions making up the spectra and the distribution function for the electric field gradient at the iron sites. We find that the Lorentz linewidth is very close to the natural linewidth of 0.2 mm/s and that the EFG distribution is both broader and more asymmetric about its peak than might be expected from dense random packing models. The EFG distribution can be fairly accurately described by an asymmetric Gaussian function and is virtually identical in shape (though not in scale) for all three materials.

---

[1] M. Henry, F. Varret, J. Teillet, G. Ferey, O. Massenet, and J. M. D. Coey, in Proceedings of the International Conference on Mössbauer Spectroscopy, Portoroz, 1979 (unpublished).

[2] J. D. Bernal, Proc. R. Soc. London Ser. A 280, 299 (1964).

[3] C. H. Bennett, J. Appl. Phys. 43, 2727 (1972).

[4] R. W. Cochrane, R. Harris, and M. Plischke, J. Non-Cryst. Solids 15, 239 (1974).

[5] M. E. Lines, Phys. Rev. B 20, 3729 (1979).

[6] M. Eibschütz, M. E. Lines, and K. Nassau, Phys. Rev. B 21, 3767 (1980).

[7] M. E. Lines, Phys. Rev. B 21, 5793 (1980).

[8] G. Czjzek, J. Fink, F. Gotz, H. Schmidt, J. M. D. Coey, J. P. Rebouillat, and A. Lienard, Phys. Rev. B 23, 2513 (1981).

[9] G. Ferey, A. M. LeClerc, R. de Pape, J. P. Mariot, and F. Varret, Solid State Commun. 29, 477 (1979).

[10] G. K. Wertheim, H. J. Guggenheim, and D. N. E. Buchanan, Phys. Rev. 169, 465 (1968).

[11] M. Eibschütz, G. R. Davidson, H. J. Guggenheim, and D. E. Cox, in *Magnetism and Magnetic Materials—1971,* edited by C. D. Graham and J. J. Rhyne, AIP Conf. Proc. No. 5 (AIP, New York, 1971), p. 670.

[12] M. Eibschütz, H. J. Guggenheim, and L. Holmes, J. Appl. Phys. 42, 1485 (1971).

[13] There is a tendency in the literature on amorphous materials to use the terms EFG distribution and Mössbauer energy distribution interchangeably. In fact they are related as in Eq. (3.2). Since the factor $(1+\eta^2/3)^{1/2}$ of this equation never deviates far from unity the two distributions for amorphous materials are virtually identical from a practical point of view except that the quadrupolar energy distribution measures only the distribution of EFG *magnitudes* and carries no information with respect to sign. In RPHS models it turns out that the EFG distribution contains roughly as many negative as positive values. Nevertheless, from the point of view of this paper only the distribution of magnitudes is relevant.

[14] See, for example, N. M. Greenwood and T. G. Gibb, in *Mössbauer Spectroscopy* (Chapman and Hall, London, 1971).

[15] J. Heberle, Nucl. Instrum. Methods 58, 90 (1968).